



Prompt η_c meson production at the LHC in the NRQCD with k_T -factorization

S. P. Baranov^{1,a}, A. V. Lipatov^{2,3,b}

¹ P.N. Lebedev Institute of Physics, Lenin Avenue 53, 119991 Moscow, Russia

² Skobeltsyn Institute of Nuclear Physics, Lomonosov Moscow State University, 119991 Moscow, Russia

³ Joint Institute for Nuclear Research, 141980 Dubna, Moscow Region, Russia

Received: 3 April 2019 / Accepted: 13 July 2019 / Published online: 25 July 2019
© The Author(s) 2019

Abstract In the framework of the k_T -factorization approach, the prompt production of η_c mesons at the LHC conditions is studied. Our consideration is based on the off-shell amplitudes for hard partonic subprocesses and on the nonrelativistic QCD (NRQCD) formalism for the formation of bound states. We try two latest parametrizations for noncollinear, or transverse momentum dependent (TMD) gluon densities derived from the Catani–Ciafaloni–Fiorani–Marchesini (CCFM) equation. We use the values of the nonperturbative matrix elements obtained from a combined fit of the η_c and J/ψ differential cross sections. Finally, we show an universal set of parameters that provides a reasonable simultaneous description for all of the available data on the prompt J/ψ and η_c production at the LHC.

1 Introduction

Since long ago, the production of quarkonium states in high energy hadronic collisions remains an area of intense attention from both theoretical and experimental sides. These processes are sensitive to the interaction dynamics both at small and large distances: the production of heavy quarks with high transverse momentum is followed by the formation of bound states with low relative quark momentum. Accordingly, the description of these processes involves both perturbative and non-perturbative methods. Our present work continues the line started in the previous publications [1–3]. We have already considered there the prompt production of ψ' , χ_c , and J/ψ mesons and now come to η_c mesons.

The production of η_c mesons turned out to be rather puzzling for conventional NRQCD calculations at the leading and next-to-leading orders (NLO) [4,5]; see also the dis-

cussions in [6–8]. This time, the theory was very unlucky to have too few degrees of freedom. The essential parameters, the so called long distance matrix elements (LDMEs) or nonperturbative matrix elements (NMEs), have been already fixed from the data on the production and polarization of J/ψ mesons. The correspondence between the η_c and J/ψ production parameters follows from the heavy quark spin symmetry rules and is explained in the next section. So, the theory lost its flexibility and made a prediction for η_c by a huge factor off the measured cross section. The overall situation was even called ‘challenging’ [4]. Large efforts invested in extending the calculations to higher orders made no sensible effect. The aim of the present note is to show that the approach consistently used in [1–3] meets no troubles with the η_c data.

Our solution implies a certain modification of the conventional NRQCD rules. We find the conventional rules rather unsatisfactory. Indeed, in all practical calculations with NRQCD, the final state gluons changing the color and other quantum numbers of the $Q\bar{Q}$ pair and bringing it to the color-singlet state are regarded as carrying no energy–momentum. This is in obvious contradiction with confinement which prohibits the emission of infinitely soft colored quanta. In reality, the heavy quark system must undergo a kind of final state interaction where the energy–momentum exchange must be larger than at least the typical confinement scale (say, Λ_{QCD}). This is not the matter of only kinematic corrections; without some finite energy–momentum transfer we cannot organise transition amplitudes with correct spin properties.

In the present work, we understand the long-distance transition amplitudes as consecutive color-electric dipole transitions in the spirit of multipole radiation theory. This has dramatic consequences for the polarization of the final state mesons. As a result of the accepted rules (see Sect. 2), the final state J/ψ mesons come out nearly unpolarized, either

^a e-mail: baranovsp@lebedev.ru

^b e-mail: lipatov@theory.sinp.msu.ru

because of the cancellation between the ${}^3P_1^{[8]}$ and ${}^3P_2^{[8]}$ contributions, or as a result of two successive color-electric (E1) dipole transitions in the chain ${}^3S_1^{[8]} \rightarrow {}^3P_J^{[8]} \rightarrow J/\psi$ with $J = 0, 1, 2$. This contrasts with the conventional NRQCD calculations which show that J/ψ mesons produced from high- p_T gluons as ${}^3P_1^{[8]}$ states carry strong transverse polarization [9]. With our completely different view on the J/ψ depolarization mechanism, we finally arrive at a completely different set of the fitted NMEs.

As usual, to preserve the consistency with our previous studies we work in the k_T -factorization approach [10–13]. The kinematics of our processes is characterized by the double inequality $s \gg \mu^2 \simeq \hat{s} \gg \Lambda^2$ which shows that the typical parton interaction scale μ is much higher than the QCD parameter Λ , but is much lower than the total c.m.s. energy \sqrt{s} . In such a case, the perturbative QCD expansions in α_s may contain large coefficients $\mathcal{O}[\ln(s/\mu^2)] = \mathcal{O}[\ln(1/x)]$ which compensate the smallness of the coupling constant $\alpha_s(\mu^2/\Lambda^2)$. Resummation of the terms $[\alpha_s \ln(\mu^2/\Lambda^2)]^n$, $[\alpha_s \ln(1/x)]^n$, and $[\alpha_s \ln(\mu^2/\Lambda^2) \ln(1/x)]^n$ up to infinitely large n results in parton distributions $\mathcal{F}_i(x, \mathbf{k}_T^2, \mu^2)$ that generalize the factorization of the hadronic matrix elements beyond the collinear approximation.

The parton evolution is described in our work with CCFM (Catani–Ciafaloni–Fiorani–Marchesini) equation [14–17]. The latter converges to BFKL (Balitsky–Fadin–Kuraev–Lipatov) equation [18–20] in the region of small x and to DGLAP equation at large x and provides a continuous interpolation between these two regimes. The typical values of x probed in the considered processes are of the order $x \sim m_T/\sqrt{s}$ with $m_T = (m^2 + p_T^2)^{1/2}$. The arguments justifying the use of CCFM equation at large x (resp., large p_T) are therefore the same as for the collinear factorization approach based on DGLAP equation. At the same time, the soft gluon resummation implemented in our parton evolution algorithm [21] regularises infrared divergences and makes our approach usable even at small p_T . For the different aspects of using the k_T -factorization approach the reader may consult the reviews [22–25].

2 Theoretical framework

As it was done previously for ψ' , χ_c and J/ψ production [1–3], the present calculations are based on perturbative QCD and nonrelativistic bound state formalism (NRQCD). The production of η_c mesons is dominated by the color singlet (CS) contribution that refers to the partonic subprocess

$$g^*(k_1) + g^*(k_2) \rightarrow \eta_c(p) \quad (1)$$

with the respective cross section

$$\begin{aligned} \sigma(pp \rightarrow \eta_c + X) &= \int \frac{2\pi}{x_1 x_2 s F} \mathcal{F}_g(x_1, \mathbf{k}_{1T}^2, \mu^2) \mathcal{F}_g(x_2, \mathbf{k}_{2T}^2, \mu^2) \\ &\times |\mathcal{M}(g^* g^* \rightarrow \eta_c)|^2 d\mathbf{k}_{1T}^2 d\mathbf{k}_{2T}^2 dy_\eta \frac{d\phi_1}{2\pi} \frac{d\phi_2}{2\pi}, \quad (2) \end{aligned}$$

where k_1 and k_2 denote the initial gluon 4-momenta, ϕ_1 and ϕ_2 are the respective azimuthal angles, y_η is the rapidity of η_c meson, x_1 and x_2 are the gluon longitudinal momentum fractions, $\mathcal{M}(g^* g^* \rightarrow \eta_c)$ is the hard scattering amplitude, and $\mathcal{F}_g(x_i, \mathbf{k}_{iT}^2, \mu^2)$ is the transverse momentum dependent (TMD, or unintegrated) gluon density in a proton at the scale μ^2 . In accordance with the general definition [26], the off-shell gluon flux factor in (2) is taken as $F = 2\lambda^{1/2}(\hat{s}, k_1^2, k_2^2)$, where $\hat{s} = (k_1 + k_2)^2$.

In addition to the above, we have considered a number of color octet (CO) contributions and a contribution from the feed-down $h_c \rightarrow \eta_c X$ process. In all of the considered cases the initial gluons are taken off-shell. That means, they have nonzero transverse momentum and an admixture of longitudinal component in the polarization vector. Explicitly, the gluon spin density matrix is taken in the form [10, 11]: $\overline{\epsilon}_g^\mu \epsilon_g^{*\nu} = k_T^\mu k_T^\nu / |k_T|^2$, where k_T is the component of the gluon momentum perpendicular to the beam axis. In the collinear limit, when $k_T \rightarrow 0$, this expression converges to the ordinary $\overline{\epsilon}_g^\mu \epsilon_g^{*\nu} = -g^{\mu\nu}/2$. In all other respects, we follow standard QCD Feynman rules.

The CO terms refer to the perturbative production of a color-octet $c\bar{c}^{[8]}$ pair followed by nonperturbative gluon radiation bringing the intermediate $c\bar{c}^{[8]}$ state to a real (colorless) meson:

$$g^*(k_1) + g^*(k_2) \rightarrow c\bar{c}^{[8]} \rightarrow \eta_c(p) + \text{soft gluons}. \quad (3)$$

The intermediate color octet $c\bar{c}^{[8]}$ state can be either of 1S_0 , 3S_1 , 3P_0 , 3P_1 , 3P_2 , or 1P_1 , where we use standard spectroscopic notation. As usual, the hard production amplitudes contain spin and color projection operators that guarantee the proper quantum numbers of the state under consideration. The probabilities of the subsequent nonperturbative soft transitions are not calculable within the theory and are usually accepted as free model parameters. There are, however, certain restrictions coming from some general principles. Whenever calculable or not, the nonperturbative amplitudes must be identical for transitions in both directions (i.e., from vectors to scalars and vice versa), as it is motivated by the heavy quark spin symmetry (HQSS). The amplitudes can only differ by an overall normalizing factor representing the averaging over spin degrees of freedom. Thus, we strictly have from this property [27, 28]:

$$\begin{aligned}
 \langle \mathcal{O}^{\eta_c} [^1S_0^{[11]}] \rangle &= \frac{1}{3} \langle \mathcal{O}^{J/\psi} [^3S_1^{[11]}] \rangle \\
 \langle \mathcal{O}^{\eta_c} [^1S_0^{[8]}] \rangle &= \frac{1}{3} \langle \mathcal{O}^{J/\psi} [^3S_1^{[8]}] \rangle \\
 \langle \mathcal{O}^{\eta_c} [^3S_1^{[8]}] \rangle &= \langle \mathcal{O}^{J/\psi} [^1S_0^{[8]}] \rangle \\
 \langle \mathcal{O}^{\eta_c} [^1P_1^{[8]}] \rangle &= 3 \langle \mathcal{O}^{J/\psi} [^3P_0^{[8]}] \rangle \\
 \langle \mathcal{O}^{h_c} [^1P_1^{[11]}] \rangle &= 3 \langle \mathcal{O}^{\chi_{c0}} [^3P_0^{[11]}] \rangle \\
 \langle \mathcal{O}^{h_c} [^1S_0^{[8]}] \rangle &= 3 \langle \mathcal{O}^{\chi_{c0}} [^3S_1^{[8]}] \rangle. \tag{4}
 \end{aligned}$$

The above relations require a simultaneous fit for the η_c and J/ψ production data. This fit turned out to be impossible in the traditional NRQCD scheme. The calculated cross sections were either found to be at odds with the measurements [4] or at odds with theoretical principles [5].

The crucial point in the above papers is the presence of a large unwanted contribution to the η_c production cross section from the intermediate $^3S_1^{[8]}$ state (unwanted, as the η_c production cross section is saturated by the color singlet channel alone; a fact, already pointed out in [29]). The corresponding nonperturbative matrix element is an HQSS counterpart of the $^1S_0^{[8]}$ matrix element engaged in the production of J/ψ mesons, where it is needed to make the outgoing J/ψ meson unpolarised: this spinless state is employed to dilute strong J/ψ polarization in other channels. Note by the way that the size of $\langle \mathcal{O}^{J/\psi} [^1S_0^{[8]}] \rangle$ matrix element used in [4] is in conflict with the NRQCD quark relative velocity counting rules.

In the present work, we exploit rather different understanding [30] of the J/ψ depolarization mechanism. This mechanism is not connected to the choice of factorization scheme (k_T or collinear), but represents a completely independent issue. We follow the interpretation of the nonperturbative matrix elements (NMEs) as consecutive color-electric dipole transitions in the spirit of multipole radiation theory.

Only a single E1 transition is needed to transform a P -wave state into an S -wave state and the structure of the respective $^3P_J \rightarrow ^3S_1 + g$ amplitudes is taken the same as for radiative decays of χ_{cJ} mesons [31, 32]:

$$\begin{aligned}
 \mathcal{A}(\chi_{c0}(p) \rightarrow J/\psi(p-k) + \gamma(k)) \\
 \propto k_\mu p^\mu \varepsilon_v^{(J/\psi)} \varepsilon_{(\gamma)}^v, \tag{5}
 \end{aligned}$$

$$\begin{aligned}
 \mathcal{A}(\chi_{c1}(p) \rightarrow J/\psi(p-k) + \gamma(k)) \\
 \propto \varepsilon^{\mu\nu\alpha\beta} k_\mu \varepsilon_v^{(\chi_{c1})} \varepsilon_\alpha^{(J/\psi)} \varepsilon_\beta^{(\gamma)}, \tag{6}
 \end{aligned}$$

$$\begin{aligned}
 \mathcal{A}(\chi_{c2}(p) \rightarrow J/\psi(p-k) + \gamma(k)) \\
 \propto p^\mu \varepsilon_{(\chi_{c2})}^{\alpha\beta} \varepsilon_\alpha^{(J/\psi)} [k_\mu \varepsilon_\beta^{(\gamma)} - k_\beta \varepsilon_\mu^{(\gamma)}]. \tag{7}
 \end{aligned}$$

The only difference is in the overall normalizing factor, as the electric charge is replaced with the color charge. The transformation of an S -wave state into another S -wave state

(such as J/ψ meson) requires two successive E1 transitions $^3S_1^{[8]} \rightarrow ^3P_J^{[8]} + g$, $^3P_J^{[8]} \rightarrow J/\psi + g$ proceeding via either of the three intermediate states: $^3P_0^{[8]}$, $^3P_1^{[8]}$, or $^3P_2^{[8]}$. Here we exploit the same effective coupling vertices as above (5)–(7) and only change the sign of the radiated momentum k for the ‘backward’ case, $^3S_1 \rightarrow ^3P_J$.

The accepted rules (5)–(7) lead to the fact that the final state J/ψ mesons come out unpolarized [30], either because of the cancellation between the $^3P_1^{[8]}$ and $^3P_2^{[8]}$ contributions, or as a result of two successive color-electric (E1) dipole transitions in the chain $^3S_1^{[8]} \rightarrow ^3P_J^{[8]} \rightarrow J/\psi$ with $J = 0, 1, 2$. Note that this property remains true irrespective of the numerical values of NMEs and only follows from the spin algebra. Thus, we no longer need the diluting $^1S_0^{[8]}$ contribution to J/ψ and can significantly reduce or even kill it. This means that we also get rid of the $^3S_1^{[8]}$ contribution to η_c production.

As we have mentioned already, our parton distribution functions are derived from CCFM equation which converges to BFKL equation at small x and to DGLAP equation at large x . We benefit from having a continuous interpolation between the two different regimes and from the ease of including radiation corrections in the form of TMD distributions. The soft gluon resummation implemented in our parton evolution algorithm regularises infrared divergences and makes our approach usable even in the low p_T region.

In the numerical analysis shown below, we tried two latest sets of TMD gluon densities in a proton, referred to as JH’2013 set 1 and JH’2013 set 2 [33]. These gluon densities were obtained from CCFM evolution equation [14–17] where the input parametrization (used as boundary conditions) was fitted to the proton structure function $F_2(x, Q^2)$. The resummation of large logarithmic terms proportional to $\ln 1/x$ (important at high energies \sqrt{s} , or, equivalently, at small $x \sim \mu/\sqrt{s}$) and $\ln 1/(1-x)$ is included in our approach as part of the CCFM evolution of gluon densities (see [14–17] for more information).

We take from [34] the charmonia masses $m(\eta_c) = 2.9839 \text{ GeV}$, $m(h_c) = 3.52538 \text{ GeV}$, $m(J/\psi) = 3.0969 \text{ GeV}$ and the branching fractions $B(J/\psi \rightarrow \mu^+\mu^-) = 0.05961$ and $B(h_c \rightarrow \eta_c\gamma) = 0.51$. The renormalization and factorization scales are set to $\mu_R^2 = m^2 + \mathbf{p}_T^2$ and $\mu_F^2 = \hat{s} + \mathbf{Q}_T^2$, where m and \mathbf{p}_T are the mass and transverse momentum of the produced charmonium, and \mathbf{Q}_T is the transverse momentum of the initial off-shell gluon pair. The choice of μ_R is rather standard for charmonia production, while the unusual choice of μ_F is connected with the CCFM evolution (see [33] for details). The analytic expressions for the hard scattering amplitudes in (1) and (3) were obtained using the algebraic manipulation system FORM [35]. The multidimensional phase space integration has been performed by means of the Monte-Carlo technique using the routine VEGAS [36].

3 Numerical results

All the J/ψ and η_c production mechanisms have different shapes of transverse momentum distributions, that enabled us to extract the corresponding NMEs from the experimental data. Here, to determine the NMEs of J/ψ mesons (as well as their η_c counterparts) we performed a combined fit of J/ψ and η_c transverse momentum distributions using the latest CMS [37,38], ATLAS [39] and LHCb data [40] collected at 7, 8 and 13 TeV. Here, the factorization principle seems to be on solid theoretical grounds because of not too low p_T values for both J/ψ and η_c mesons. We do not impose any kinematic restrictions but the experimental acceptance. The fitting procedure was separately done (using fitting algorithm as implemented in GNUPLOT package [41]) in each of the rapidity subdivisions under the requirement that the NMEs be strictly positive, and then the mean-square average of the fitted values was taken. The corresponding uncertainties are estimated in a standard way using Student's t-distribution at confidence level $P = 95\%$. Note that we used the results of a global fit for the entire charmonium family (including, in particular, χ_{cJ} and ψ' states) [44] to properly calculate the feed-down contributions from h_c , χ_{cJ} , and ψ' decays.

For some (yet unrecognized) reasons, our $^1P_1^{[1]}$ production amplitude (needed to calculate the feed-down $h_c \rightarrow \eta_c X$) disagrees with the one found in the literature. Our calculation is off-shell, but has continuous on-shell limit that can be promptly compared with [45,46]. The contribution is anyway small and unimportant numerically; but the discrepancy is still of interest from the academic point of view. For the lack of details presented in [45,46], we cannot repeat their calculation. The details of our calculation are explained in the Appendix.

The numerical values of our NMEs for J/ψ and h_c mesons are written out in Tables 1 and 2. For comparison, we also present here several sets of NMEs [42,43,47,48], obtained in the NLO NRQCD by other authors. The NMEs shown for h_c mesons are translated from χ_c NMEs using HQSS formulas. The fits differ from one another by somehow differently selected data sets. The corresponding values of NMEs for η_c meson are collected in Table 3. They can be easily obtained from Table 1 using the HQSS relations (4).

A comparison of our predictions with the experimental results is displayed in Figs. 1 and 2. The theoretical uncertainty bands include both scale uncertainties and the uncertainties coming from the NMEs fitting procedure. First of them were obtained by varying the μ_R scale around its default

Table 1 Sets of NME's for J/ψ production as determined from the different fits

	JH set 1	JH set 2	Kniehl et al. [42]	Gong et al. [43]
$\langle \mathcal{O}^{J/\psi} [^3S_1^{[1]}] \rangle / \text{GeV}^3$	1.16	1.16	1.32	1.16
$\langle \mathcal{O}^{J/\psi} [^1S_0^{[8]}] \rangle / \text{GeV}^3$	0.0	0.0	0.304	0.097
$\langle \mathcal{O}^{J/\psi} [^3S_1^{[8]}] \rangle / \text{GeV}^3$	$(4.2 \pm 0.9) \times 10^{-4}$	$(1.6 \pm 0.2) \times 10^{-3}$	0.00168	-0.0046
$\langle \mathcal{O}^{J/\psi} [^3P_0^{[8]}] \rangle / \text{GeV}^5$	0.023 ± 0.002	0.024 ± 0.002	-0.00908	-0.0214

Table 2 Sets of NME's for h_c production as determined from the different fits

	JH set 1	JH set 2	Zhang et al. [47]	Likhoded et al. [48]
$\langle \mathcal{O}^{h_c} [^1P_1^{[1]}] \rangle / \text{GeV}^5$	3.1 ± 0.4	3.2 ± 0.5	0.96	4.51
$\langle \mathcal{O}^{h_c} [^1S_0^{[8]}] \rangle / \text{GeV}^3$	$(6.0 \pm 3.0) \times 10^{-4}$	$(1.5 \pm 0.9) \times 10^{-3}$	0.00603	0.00132

Table 3 Sets of NME's for η_c production as determined from the different fits

	JH set 1	JH set 2	Kniehl et al. [42]	Gong et al. [43]
$\langle \mathcal{O}^{\eta_c} [^1S_0^{[1]}] \rangle / \text{GeV}^3$	0.39	0.39	0.44	0.39
$\langle \mathcal{O}^{\eta_c} [^3S_1^{[8]}] \rangle / \text{GeV}^3$	0.0	0.0	0.304	0.097
$\langle \mathcal{O}^{\eta_c} [^1S_0^{[8]}] \rangle / \text{GeV}^3$	$(1.4 \pm 0.3) \times 10^{-4}$	$(5.3 \pm 0.7) \times 10^{-4}$	0.00056	-0.0015
$\langle \mathcal{O}^{\eta_c} [^1P_1^{[8]}] \rangle / \text{GeV}^5$	0.069 ± 0.006	0.072 ± 0.006	-0.02724	-0.0642

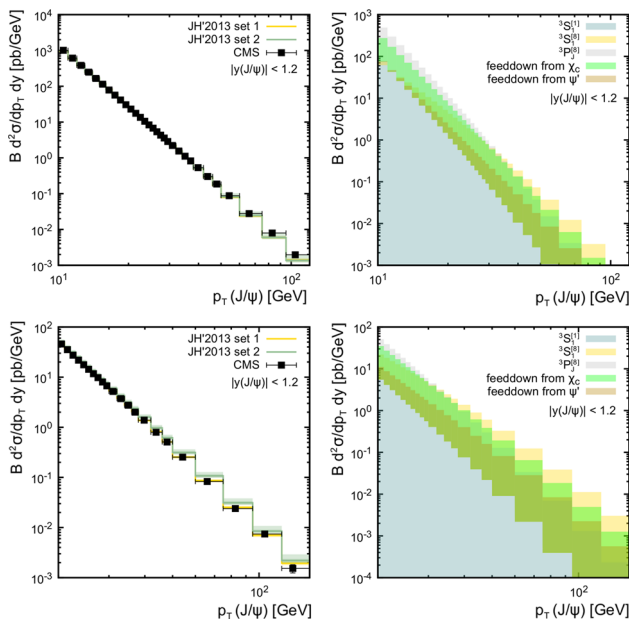


Fig. 1 Transverse momentum distribution of prompt J/ψ mesons produced in pp collisions at $\sqrt{s} = 7$ TeV (upper plots) and $\sqrt{s} = 13$ TeV (lower plots). The shaded bands on the left panels represent the total uncertainties of our calculations (i.e. scale uncertainties and the uncertainties coming from NMEs fit, summed in quadrature), as estimated for JH’2013 set 2 gluon density. The relative contributions from the different production mechanisms are shown on the right panels. The experimental data are from CMS [37, 38]

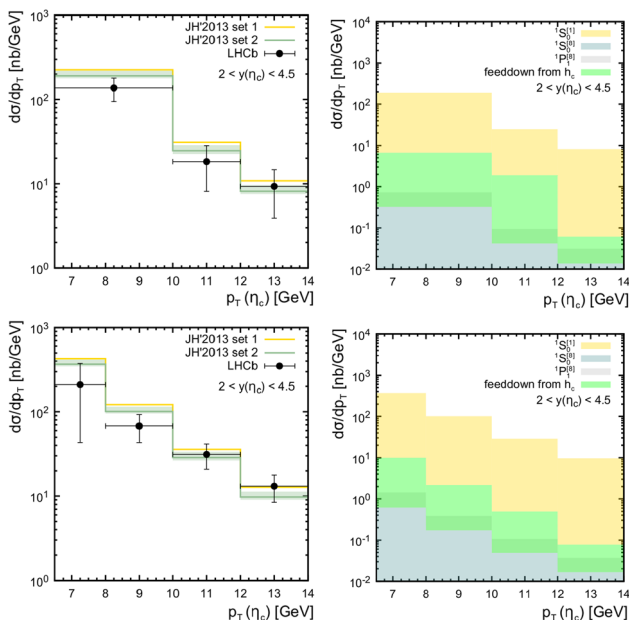


Fig. 2 Transverse momentum distribution of prompt η_c mesons produced in pp collisions at $\sqrt{s} = 7$ TeV (upper plots) and $\sqrt{s} = 8$ TeV (lower plots). Shaded bands on the left panels represent the total uncertainties of our calculations (i.e. scale uncertainties and the uncertainties coming from NMEs fit, summed in quadrature), as estimated for JH’2013 set 2 gluon density. The relative contributions from the different production mechanisms are shown on the right panels. The experimental data are from LHCb [40]

value by a factor of 2. This was accompanied with using the JH’2013 set 2+ and JH’2013 set 2– in place of the JH’2013 set 2, in accordance with [33]. One can see that we have achieved a reasonably good agreement between our calculations and LHCb measurements (with both of the considered TMD gluons), simultaneously for the prompt η_c and J/ψ production data collected at different energies and in the whole p_T range. The presented results can give a significant impact on the understanding of charmonia production within NRQCD.

4 Conclusions

We have considered the production of charmonium states at the LHC and found a consistent simultaneous description for the J/ψ and η_c data. Our fitted nonperturbative matrix elements are universal and strictly obey the heavy quark spin symmetry rules.

The fundamental difference with the ‘traditional’ NRQCD scheme (which was unable to accommodate the whole data set) is in a different treatment of the nonperturbative color-octet transitions. The latter are described in our approach in terms of multipole radiation theory. Then the J/ψ mesons are produced nearly unpolarized in all channels, thus making no special need in the diluting $^1S_0^{[8]}$ contribution to J/ψ production and, accordingly, requiring no $^3S_1^{[8]}$ contribution to η_c production. In the forthcoming paper [44] we are going to present a global fit for the entire charmonium family, including J/ψ , χ_{cJ} , $\psi(2S)$ and η_c mesons.

Acknowledgements We would like to thank H. Jung for his interest, very useful discussions and important remarks. This work was supported by the DESY Directorate in the framework of Moscow-DESY project on Monte Carlo implementations for HERA-LHC.

Data Availability Statement This manuscript has no associated data or the data will not be deposited. [Authors’ comment: There are no external data associated with the manuscript.]

Open Access This article is distributed under the terms of the Creative Commons Attribution 4.0 International License (<http://creativecommons.org/licenses/by/4.0/>), which permits unrestricted use, distribution, and reproduction in any medium, provided you give appropriate credit to the original author(s) and the source, provide a link to the Creative Commons license, and indicate if changes were made. Funded by SCOAP³.

Appendix: Off-shell production amplitude for $^1P_1^{[1]}$ state

In this section, we consider the gluon–gluon fusion subprocess

$$g(k_1, \epsilon_1, a) + g(k_2, \epsilon_2, b) \rightarrow g(k_3, \epsilon_3, c) + c\bar{c}(p, \epsilon^\alpha), \quad (8)$$

where the symbols in the parentheses indicate the momentum, the polarization, and the color of the interacting quanta. The calculation of this subprocess at $\mathcal{O}(\alpha_s^3)$ relates to six Feynman diagrams:

$$\mathcal{M}_1 = \text{tr}\{\not{\epsilon}_1(\not{p}_c - \not{k}_1 + m_c) \not{\epsilon}_2(-\not{p}_{\bar{c}} - \not{k}_3 + m_c) \not{\epsilon}_3 \mathcal{P}_S\} \times [k_1^2 - 2(p_c k_1)]^{-1} [k_3^2 + 2(p_{\bar{c}} k_3)]^{-1}, \tag{9}$$

$$\mathcal{M}_2 = \text{tr}\{\not{\epsilon}_1(\not{p}_c - \not{k}_1 + m_c) \not{\epsilon}_3(-\not{p}_{\bar{c}} + \not{k}_2 + m_c) \not{\epsilon}_2 \mathcal{P}_S\} \times [k_1^2 - 2(p_c k_1)]^{-1} [k_2^2 - 2(p_{\bar{c}} k_2)]^{-1}, \tag{10}$$

$$\mathcal{M}_3 = \text{tr}\{\not{\epsilon}_3(\not{p}_c + \not{k}_3 + m_c) \not{\epsilon}_1(-\not{p}_{\bar{c}} + \not{k}_2 + m_c) \not{\epsilon}_2 \mathcal{P}_S\} \times [k_3^2 + 2(p_c k_3)]^{-1} [k_2^2 - 2(p_{\bar{c}} k_2)]^{-1}, \tag{11}$$

$$\mathcal{M}_4 = \text{tr}\{\not{\epsilon}_2(\not{p}_c - \not{k}_2 + m_c) \not{\epsilon}_1(-\not{p}_{\bar{c}} - \not{k}_3 + m_c) \not{\epsilon}_3 \mathcal{P}_S\} \times [k_2^2 - 2(p_c k_2)]^{-1} [k_3^2 + 2(p_{\bar{c}} k_3)]^{-1}, \tag{12}$$

$$\mathcal{M}_5 = \text{tr}\{\not{\epsilon}_2(\not{p}_c - \not{k}_2 + m_c) \not{\epsilon}_3(-\not{p}_{\bar{c}} + \not{k}_1 + m_c) \not{\epsilon}_1 \mathcal{P}_S\} \times [k_2^2 - 2(p_c k_2)]^{-1} [k_1^2 - 2(p_{\bar{c}} k_1)]^{-1}, \tag{13}$$

$$\mathcal{M}_6 = \text{tr}\{\not{\epsilon}_3(\not{p}_c + \not{k}_3 + m_c) \not{\epsilon}_2(-\not{p}_{\bar{c}} + \not{k}_1 + m_c) \not{\epsilon}_1 \mathcal{P}_S\} \times [k_3^2 + 2(p_c k_3)]^{-1} [k_1^2 - 2(p_{\bar{c}} k_1)]^{-1}, \tag{14}$$

$$\mathcal{M} = \mathcal{M}_1 + \mathcal{M}_2 + \mathcal{M}_3 + \mathcal{M}_4 + \mathcal{M}_5 + \mathcal{M}_6, \tag{15}$$

with the property $\mathcal{M}_1 = \mathcal{M}_6, \mathcal{M}_2 = \mathcal{M}_5, \mathcal{M}_3 = \mathcal{M}_4$. The color factor is universal and is equal to $d^{abc}/4\sqrt{3}$. This set of diagrams is complete; no other diagrams can contribute at the order $\mathcal{O}(\alpha_s^3)$ to the production of a meson with the given quantum numbers $J^{PC} = 1^{+-}$.

The amplitudes \mathcal{M}_i contain spin projection operators which discriminate the spin-singlet and spin-triplet $c\bar{c}$ states:

$$\mathcal{P}_{S=0} = (\not{p}_{\bar{c}} - m_c)\gamma_5(\not{p}_c + m_c) \cdot (2m_c)^{-3/2}, \tag{16}$$

$$\mathcal{P}_{S=1} = (\not{p}_{\bar{c}} - m_c) \not{\psi}(\not{p}_c + m_c) \cdot (2m_c)^{-3/2}, \tag{17}$$

where m_c is the charmed quark mass. These projectors are orthogonal to each other, as they should be: $\text{tr}\{\mathcal{P}_0 \overline{\mathcal{P}}_1\} = 0$. For the $^1P_1^{11}$ state we evidently have to use the projector \mathcal{P}_0 .

The orbital angular momentum L is associated with the relative momentum q of the quarks in a bound state. The relative momentum q is defined as

$$p_c = \frac{1}{2}p + q, \quad p_{\bar{c}} = \frac{1}{2}p - q. \tag{18}$$

According to a general formalism developed in [49,50], the terms showing no dependence on q are identified with the contributions to the $L = 0$ state; the terms linear in q^α are related to the $L = 1$ state with the proper polarization vector ϵ^α (see below); the quadratic terms $q^\alpha q^\beta$ refer to the $L = 2$ state with the polarization tensor $\epsilon^{\alpha\beta}$; and so on. The decomposition of \mathcal{M} in powers of q is carried out by expanding the subprocess amplitude as

$$\mathcal{M}(q) = \mathcal{M}|_{q=0} + q^\alpha (\partial \mathcal{M} / \partial q^\alpha)|_{q=0} + \dots, \tag{19}$$

where q is assumed to be a small quantity. The amplitude $\mathcal{M}(q)$ has to be multiplied by the bound state wave function $\Psi(q)$ and integrated over q . A term-by-term integration of Eq.(19) is performed using the relations

$$\int \frac{d^3q}{(2\pi)^3} \Psi(q) = \frac{1}{\sqrt{4\pi}} \mathcal{R}(x=0), \tag{20}$$

$$\int \frac{d^3q}{(2\pi)^3} q^\alpha \Psi(q) = -i\epsilon^\alpha \frac{\sqrt{3}}{\sqrt{4\pi}} \mathcal{R}'(x=0), \tag{21}$$

etc., where $\mathcal{R}(x)$ is the radial wave function in the coordinate representation (the Fourier transform of $\Psi(q)$). This formula completes our derivation of the production matrix element. The resulting expression has been explicitly tested for gauge invariance by substituting the gluon momentum k_i for the polarization vector ϵ_i . We have observed gauge invariance even with off-shell initial gluons.

References

1. S.P. Baranov, A.V. Lipatov, N.P. Zotov, Eur. Phys. J. C **75**, 455 (2015)
2. S.P. Baranov, A.V. Lipatov, N.P. Zotov, Phys. Rev. D **93**, 094012 (2016)
3. S.P. Baranov, A.V. Lipatov, Phys. Rev. D **96**, 034019 (2017)
4. M. Butenshoen, Z.-G. He, B.A. Kniehl, Phys. Rev. Lett. **114**, 092004 (2015)
5. H. Han, Y.-Q. Ma, C. Meng, H.-S. Shao, K.-T. Chao, Phys. Rev. Lett. **114**, 092005 (2015)
6. J.-P. Lansberg, H.-S. Shao, H.-F. Zhang, Phys. Lett. B **786**, 342 (2018). [arXiv:1711.00265](https://arxiv.org/abs/1711.00265) [hep-ph]
7. Y. Feng, J. He, J.-P. Lansberg, H.-S. Shao, A. Usachov, H.-F. Zhang., Nucl. Phys. B **945**, 114662 (2019)
8. J.-P. Lansberg. [arXiv:1903.09185](https://arxiv.org/abs/1903.09185) [hep-ph]
9. K.-T. Chao, Y.-Q. Ma, H.-S. Shao, K. Wang, Y.-J. Zhang, Phys. Rev. Lett. **102**, 242004 (2012)
10. L.V. Gribov, E.M. Levin, M.G. Ryskin, Phys. Rep. **100**, 1 (1983)
11. E.M. Levin, M.G. Ryskin, YuM Shabelsky, A.G. Shuvaev, Sov. J. Nucl. Phys. **53**, 657 (1991)
12. S. Catani, M. Ciafaloni, F. Hautmann, Nucl. Phys. B **366**, 135 (1991)
13. J.C. Collins, R.K. Ellis, Nucl. Phys. B **360**, 3 (1991)
14. M. Ciafaloni, Nucl. Phys. B **296**, 49 (1988)
15. S. Catani, F. Fiorani, G. Marchesini, Phys. Lett. B **234**, 339 (1990)
16. S. Catani, F. Fiorani, G. Marchesini, Nucl. Phys. B **336**, 18 (1990)
17. G. Marchesini, Nucl. Phys. B **445**, 49 (1995)
18. E.A. Kuraev, L.N. Lipatov, V.S. Fadin, Sov. Phys. JETP **44**, 443 (1976)
19. E.A. Kuraev, L.N. Lipatov, V.S. Fadin, Sov. Phys. JETP **45**, 199 (1977)
20. I.I. Balitsky, L.N. Lipatov, Sov. J. Nucl. Phys. **28**, 822 (1978)
21. H. Jung et al., Eur. Phys. J. C **70**, 1237 (2010)
22. B. Andersson et al. (Small-x Collaboration), Eur. Phys. J. C **25**, 77 (2002)
23. J. Andersen et al. (Small-x Collaboration), Eur. Phys. J. C **35**, 67 (2004)
24. J. Andersen et al. (Small-x Collaboration), Eur. Phys. J. C **48**, 53 (2006)

25. R. Angeles-Martinez et al., *Acta Phys. Polon. B* **46**, 2501 (2015)
26. E. Bycling, K. Kajantie, *Particle Kinematics* (Wiley, New York, 1973)
27. G.T. Bodwin, E. Braaten, G.P. Lepage, *Phys. Rev. D* **51**, 1125 (1995)
28. G.T. Bodwin, E. Braaten, G.P. Lepage, *Phys. Rev. D* **55**, 5853(E) (1997)
29. A.K. Likhoded, A.V. Luchinsky, S.V. Poslavsky, *Mod. Phys. Lett. A* **30**, 1550032 (2015)
30. S.P. Baranov, *Phys. Rev. D* **93**, 054037 (2016)
31. A.V. Batunin, S.R. Slabospitsky, *Phys. Lett. B* **188**, 269 (1987)
32. P. Cho, M. Wise, S. Trivedi, *Phys. Rev. D* **51**, R2039 (1995)
33. F. Hautmann, H. Jung, *Nucl. Phys. B* **883**, 1 (2014)
34. Particle Data Group, *Chin. Phys. C* **40**, 100001 (2016)
35. J.A.M. Vermaseren, *Symbolic Manipulations with FORM* (Computer Algebra Nederland, Amsterdam, 1991). (ISBN 90-74116-01-9)
36. G.P. Lepage, *J. Comput. Phys.* **27**, 192 (1978)
37. CMS Collaboration, *Phys. Rev. Lett.* **114**, 191802 (2015)
38. CMS Collaboration, *Phys. Lett. B* **780**, 251 (2018)
39. ATLAS Collaboration, *Eur. Phys. J. C* **76**, 47 (2016)
40. LHCb Collaboration, *Eur. Phys. J. C* **75**, 311 (2015)
41. GNUPLOT package. <http://www.gnuplot.info>
42. M. Butenshoen, B.A. Kniehl, *Phys. Rev. D* **84**, 051501(R) (2011)
43. B. Gong, L.-P. Wan, J.-X. Wang, H.-F. Zhang, *Phys. Rev. Lett.* **110**, 042002 (2013)
44. S.P. Baranov, A.V. Lipatov (2019). [arXiv:1906.07182](https://arxiv.org/abs/1906.07182) [hep-ph]
45. M.M. Meijer, J. Smith, W.L. van Neerven, *Phys. Rev. D* **77**, 034014 (2008). [arXiv:0710.3090](https://arxiv.org/abs/0710.3090)
46. R. Gastmans, W. Troost, T.T. Wu, *Nucl. Phys. B* **291**, 731 (1987)
47. H.-F. Zhang, L. Yu, S.-X. Zhang, L. Jia, *Phys. Rev. D* **93**, 054033 (2016)
48. A.K. Likhoded, A.V. Luchinsky, S.V. Poslavsky, *Phys. Rev. D* **90**, 074021 (2014)
49. H. Krasemann, *Z. Phys. C* **1**, 189 (1979)
50. G. Guberina, J. Kühn, R. Peccei, R. Rückl, *Nucl. Phys. B* **174**, 317 (1980)